Journal of Applied Fluid Mechanics , Vol. 9, No. 4, pp. 1731-1743, 2016.
Available online at www.jafmonline.net, ISSN 1735-3572, EISSN 1735-3645.
DOI: 10.18869/acadpub.jafm.68.235.24510

On the Linear Stability of Thermal Convection with Three Different Imposed Shear Flows

I. Pérez-Reyes

Facultad de Ciencias Químicas, Universidad Autónoma de Chihuahua, Circuito Universitario 1, Nuevo Campus Universitario, Chihuahua, Chih., 31125 México

Corresponding Author Email: *ildebrando3@gmail.com*

(Received January, 14, 2015; accepted September, 1, 2015)

ABSTRACT

The problem of convection in a fluid with temperature dependent viscosity and imposed shear flow, driven by pressure gradients and by a top moving wall, is studied for the case of poorly thermal conducting horizontal walls. Analytical expressions accounting for temperature dependent viscosity effects were obtained for the critical Rayleigh number and frequency of oscillation under a shallow water approximation for Poiseuille, Couette and returning primary flows. The results of this investigation contirbute and extend previous findings showing that the onset of convection can be achieved at smaller critical Rayleigh and wavenumbers. The results include approximations of weak and strong shear flows along with conditions for rigid-rigid and rigid-free boundaries. It was found that the imposed shear flow does not influence the critical wavenumber but it does increases the critical Rayleigh number. In this case convection sets in as oscillatory.

Keywords: Temperature dependent viscosity; Shallow water approximation; Returning flow.

NOMENCLATURE

B	Biot number
c	criticality
H	fluid layer depth
K	non-Boussinesq coefficient
k	wavenumber
L	lower boundary
Pr	Prandtl number
p	pressure
Ra	Rayleigh number
Re	Reynolds number
U	upper boundary
U_{max}	maximum velocity
$\mathbf{u}$	fluid velocity
W	vertical velocity component
x, y	horizontal coordinates
z	vertical coordinate
Pr	Prandtl number
γ	angle of orientation
θ	temperature
κ	thermal diffusivity
μ_0	dynamic viscosity
ν_0	kinematic viscosity
σ_R	perturbation growth rate
ω	frequency of oscillation
Subscripts	
0	basic state
1	perturbation variable
Superscripts	
$*$	dimensional form
Tr	transpose operation

1. INTRODUCTION

Convective hydrodynamic stability in a horizontal fluid layer is calling the attention of experimentalists since this is an alternative to the fabrication of corrugated surfaces with convective patterns (Nie 2008; Bassou 2009; Sakurai *et al.* 2002; Xu 2002; Li *et al.* 2000; Li *et al.* 2000). In these experimental investigations convective patterns such as hexagonal cells are induced and deposited by evaporation of the solvent in a layer of polymeric solution. The resulting patterned surfaces are of technological interest for the fabrication of light emitting displays and semiconductor electronics among others (Nie 2008).

The present investigation is intended to give theoretical insight about possible experimental conditions. These results are also of interest to several fields such as in the context of atmospheric studies, geophysics (Kameyama *et al.* 2013; Landuyt and Ierley 2012; Höink and Lenardic 2010), oceanography, solidification processes in metallurgy (Lappa 2010) and several problems involving long-wavelength thermal convection (Uguz and Narayanan 2012; Landuyt and Ierley 2012). Some other applications are those of control of convection in which not only the properties of the bounding walls are important but also those of the working fluid (Khalid, Mokhar, and Arifin 2013; Howle 2000; Tang and Bau 1998; Howle 1997a; Howle 1997b; Tang and Bau 1994; Tang and Bau 1993). In applications like drying of thin films, patterns may arise (Schwartz *et al.* 2001) and then the proper understanding and control of convection becomes important.

Here, the onset of thermal convection in the presence of a principal shear flow in a horizontal fluid layer bounded by two poorly conducting boundaries is studied. Results of the linear stability analysis are exposed, showing analytical expressions for the critical Rayleigh number Ra_c, and the critical frequency of oscillation ω_c accounting for three different parallel shear flows as well.

This theoretical investigation was performed analytically in order to clarify to some extent the behaviour and role of the parameters appearing in this problem. Although non-linear hydrodynamic studies are very common nowadays, it should be noted the importance of the linear stability analysis problem. In one hand, several investigations are mostly concerned with the setting in of convective patterns and then the results of the linear hydrodynamic stability analysis play a key role. On the other hand, in weakly non-linear stability situations were the behaviour of the system is studied a little far from criticality, the linear stability analysis is also relevant. Thus, the linear stability analysis is an important first step before any more complete non-linear hydrodynamic stability investigation.

In this work some modifications and extensions are made to reported results in the literature related to this problem. A returning flow is included as another possible parallel flow in shallow water conditions. The returning flow arises in this case in the middle region of a very long shallow cavity. A shallow cavity is one with small depth. In the literature, to the best knowledge of the author, this parallel flow was firstly reported by Weber (1973) arising from the combination of horizontal and vertical temperature gradients. More recently, Ortiz–Pérez and Dávalos–Orozco (2014), Alloui *et al.* (2013) and Ortiz–Pérez and Dávalos–Orozco (2011) reported results of the thermoconvective stability in a cavity where similar returning flows arise too.

Several scenarios were considered for the study of the thermal instability of a horizontal fluid layer. First, a situation with both solid bounding walls is studied with the upper wall moving in a horizontal direction. Another situation considers fixed lower solid bounding wall and upper free boundary. In combination with these physical constraints yet the shear flow is tuned as weak for flows with small Reynolds number Re and as strong for flows with $Re = O(1)$.

The problem of the linear thermoconvective stability of a Boussinesq fluid have been widely studied since several years ago for a number of cases. Important results were provided by Chapman and Proctor (1980a) and by Busse and Riahi (1980) for the case of natural convection of a Boussinesq fluid layer confined between two poorly conducting boundaries, and by Chapman and Proctor (1980b) for a fluid layer confined between two non-conducting boundaries. Alikina and Tarunin (2001) investigated subcritical convective motion in a fluid with temperature dependent viscosity by means of numerical experiments. Some other conditions have also been included to this kind of problem making it more real and reproducible in the laboratory. A wide review on the forced convection in Boussinesq fluids have been published by Nicolas (2002) with applied Couette and Poisueuille flow in ducts heated from below. Very interesting results have been reported by Bessonov *et al.* (1998) about fluid motions driven by a lid in cavity. Also, results on the coupled stability problem of a parallel flow and thermal convection in an elongated cavity have been reported by Nikitin *et al.* (1996). Cox (1996) reported results for forced convection in fluids with high Prandtl Pr numbers and poorly conducting boundaries. Recently Sassos and Pantokratoras (2011) reported numerical computations for Rayleigh convection with all fluid properties variable. The heat transfer in hydromagnetic fluids with temperature dependence of viscosity has also been investigated by Ghosh *et al.* (2014) and Molla *et al.* (2012). For fluids with slightly temperature dependent viscosity interesting findings have been reported too. Cox (1997) obtained results on the linear and

non-linear hydrodynamic convective stability in a horizontal fluid layer in presence of Couette and Poiseuille flow and with the kinematic viscosity as a linear function of the temperature. Surprisingly, in the linear stability results of Cox (1997) the effects of small variations of viscosity with temperature are not present and arise only as non-linearities. In an earlier non-linear stability investigation Palm *et al.* (1967) also considered linear variations of viscosity with temperature in the Rayleigh convection. However, Palm *et al.* (1967) took into account perfectly thermal conducting walls. From a comparison of working Eq. (4a) in the paper of Cox (Cox 1997) and Eqs. (2.1) and (2.10) in the paper of Palm *et al.* (1967) it can be noted that linear and non-linear terms are missing in the equations of Cox (1997). This investigation takes into account these contributions to the linear stability case and shows that slight temperature dependent viscosity effects may contribute to the linear thermoconvective instability of the fluid layer. The linear stability problem is revisited and expanded to include modifications in the parallel flows as well.

The paper is organized as follows. In section 2., the mathematical formulation of the problem is stated providing the boundary conditions, velocity profiles and non-dimensionalization. The linear stability analysis is presented in section 3. exposing the mathematical treatment. In section 4., results and a brief insight on non-linear consequences of the present theory is given. Finally, conclusions are outlined in section 5..

2. MATHEMATICAL FORMULATION

The present problem of forced convection is now described. Lets consider an infinite horizontal fluid layer in the plane x^*y^* and of depth H in the $z^* - axis$ as shown in Fig. 1. The working fluid, heated from below with $T_L > T_U$, is Newtonian, incompressible and has slightly temperature dependent viscosity. In the scheme shown in Fig. 1. the top wall may be either rigid or free as needed to represent both possibilities rigid-rigid and rigid-free boundary conditions. The scheme in Fig. 1. also shows the situation of thermal convection in the presence of returning flow, where only the middle region far from the lateral walls is of interest in this study. The lower and upper walls are nearly thermal insulators and, as mentioned above, the viscosity of the fluid is a function of temperature $\mu(T^*)$. The problem is made non-dimensional according to the following scales: H for legth, κ/H for velocity, $\kappa\mu_0/H^2$ for pressure, ΔT^* for temperature and H^2/κ for time. The function $\mu(T^*)$

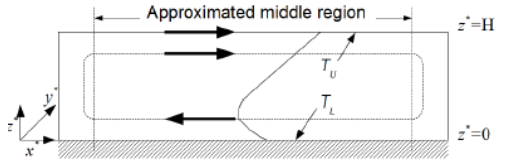

Fig. 1. Fluid layer arrangement for the returning flow case in very long shallow cavity. The flow is considered to be parallel in the middle region indicated by vertical doted lines.

must be taken into account in the stress tensor. This, process have been implemented before by Wall and Wilson (1996) and Chung and Wulandana (2006) in the stability analysis of heated parallel flows through channels. In the work of Wall and Wilson (1996) and Chung and Wulandana (2006) is noticeable that common Poiseuille flow is modified and the resulting velocity profile is skewed towards one of the walls. Thus,

$$\tau^* = -p^* I + 2\mu(T^*)\left(\frac{1}{2}\left[\nabla \mathbf{u}^* + (\nabla \mathbf{u}^*)^{Tr}\right]\right) \quad (1)$$

where the superscript $*$ indicates dimensionless variables and the superscript Tr stands for transpose operation. The governing equations for this problem are the continuity equation, the Navier-Stokes equations and the heat equation. This system of equations is perturbed according to,

$$\mathbf{u}^* = \mathbf{u}_0^* + \varepsilon \mathbf{u}_1^* \quad (2)$$

$$T^* = T_0^* + \varepsilon T_1^* \quad (3)$$

$$p^* = p_0^* + \varepsilon p_1^* \quad (4)$$

where $\varepsilon << 1$ and is defined later in terms of the Biot number. Here $\mathbf{u}_0^*$, T_0^* and p_0^* are de basic profiles for the velocity, temperature and pressure, respectively. For temperature it is $T_0^* = -(T_L - T_U)z^*/H + T_L^*$. Using the same idea of Wall and Wilson (1996) and Chung and Wulandana (2006) a linear temperature dependence of viscosity is considered. Thus,

$$\nu(T^*) = \nu_0\left(1 + K\frac{T^* - T_L^*}{\Delta T}\right) \quad (5)$$

where ν_0 is a viscosity of reference and K is a coefficient that accounts for the temperature dependence of viscosity. This is, when $K = 0$ the viscosity ν is temperature independent and temperature dependent if $K > 0$. The velocity profiles differ from those arising in the work of

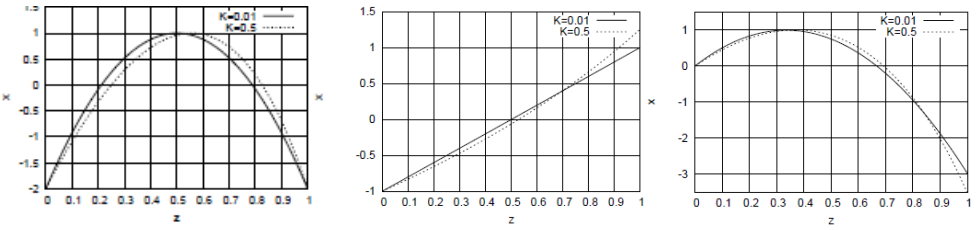

(a) Modified Poiseuille flow (b) Modified Couette flow (c) Modified return flow

Fig. 2. Curves of the modified Poiseuille flow (Eq. 48), modified Couette flow (Eq. 51) and modified return flow (Eq. 53) for two different values *K* accounting for the effect of the temperature on the fluid viscosity.

Cox (1997) since thermal variations in the viscosity modify the equation for the primary flow $\mathbf{u}_0 = u_0(z)^*\mathbf{i}$ as follows,

$$\left(1+K\frac{z^*}{H}\right)\frac{d^2u_0^*}{dz^2}-\frac{K}{H}\frac{du_0^*}{dz}=\frac{1}{\mu_0}\frac{dp_0}{dx} \tag{6}$$

Eq. 6 is in agreement with that reported by Chung and Wulandana (2006), Wall and Nagata (2000) and Wall and Wilson (1996) which appears in the stability of flows with temperature dependent viscosity. The solution to Eq. 6 is,

$$u_0^*=\frac{\alpha H z^*}{K\mu_0}-\frac{\ln\left(H-Kz^*\right)}{K}C_1 + \frac{\ln\left(H-Kz^*\right)H^2\alpha}{K^2\mu_0}+C_2 \tag{7}$$

where the constants of integration, C_1 and C_2, are calculated with the help of mechanical boundary conditions which depend on the physical situation considered. The three different mechanisms driving the flow: horizontal pressure gradient, upper moving wall and upper moving wall in a very long shallow cavity, were considered to find C_1 and C_2 for rigid-rigid and rigid-free boundary conditions. Although, the full set of boundary conditions applied to find C_1 and C_2 are not explicitly given, note for future reference that these are the same used for Poiseuille, Couette and returning flow. It is noticeable from Fig. 2. that the temperature dependence of viscosity may skew the velocity profiles for different values of K. It was also found that the higher the value of K the stronger the skew towards one of the walls in the profile. This behavior was expected since between the bottom and top walls there is a temperature gradient which modifies the fluid viscosity. As a consequence near the bottom wall the fluid viscosity is decreased and buoyancy effects are increased. This is because the viscous forces are smaller near the bottom than for the case of constant viscosity. The resulting velocity profiles are not presented in this section but given in the Appendix A. Since K is interpreted as a coefficient accounting for the temperature dependence of viscosity and only small temperature effects are investigated, $K = O(\varepsilon)$ was taken. Thus, the influence of K in u_0^* is slight and all velocity profiles, shown in the Appendix A, can be approximated to the following general form,

$$\mathbf{u_0} = u_0(z)\mathbf{i} = PrRe\left[\left(\beta_1 z^2+\delta_1 z+\eta_1\right) +\varepsilon\bar{K}\left(\beta_2 z^3+\delta_2 z^2+\eta_2 z+\phi_2\right)\right] \tag{8}$$

where all variables are now in non-dimensional form. All velocity profiles were scaled with the maximum velocity U_{max} so that the Reynolds number is defined as $Re = HU_{max}/\nu_0$. Also, the averages of the basic velocities Eq. 8 over the fluid layer depth vanish. Table 1 shows the values β_1, δ_1 and η_1 while the values for β_2, δ_2 η_2 and ϕ_2 are presented in separated table in the Appendix A. As mentioned early the parallel flows are similar to that of Poiseuille, Couette and returning flow but not equal. Therefore, the one driven by a pressure gradient, an upper moving wall and an upper moving wall in a very long shallow cavity shall be named Modified Poiseuille Flow (MPF), Modified Couette Flow (MCF) and Modified Returning Flow (MRF), respectively.

Figure 2 shows the graphical representation of Eq. 8 for the case of both rigid bounding surfaces. In order to obtain the curves in Figs. 2a-2c the data of Tables 1 and 2 should be used. These curves clearly show the effect of linear temperature dependence of viscosity. Notice, that this represents an extension to the previous work of Cox (1997). When $K = 0.01$ the velocity profiles do not show graphical difference with the traditional Poiseuille, Couette and return parallel flows but when the temperature ef-

fect is increased as $K = 0.5$ the curves change notoriously. An important fact is that the flow symmetry is broken. For example, the Couette flow profile is not linear anymore as shown in Fig. 2b.

The non-dimensional temperature profile is $T_0(z) = -z + T_L/(T_L - T_U)$. Next, the governing equations may be stated in terms of the perturbed variables Eq. 2. Thus, for the linear stability at $O(\varepsilon)$ the following perturbed equations for momentum, continuity and heat are obtained,

$$Pr^{-1}\left[\frac{\partial \mathbf{u}_1}{\partial t} + PrRe\left(u_0\frac{\partial \mathbf{u}_1}{\partial x} + w_1\frac{\partial \mathbf{u}_0}{\partial z}\right)\right] = -\nabla p_1 + KPrReT_1\frac{d^2\mathbf{u}_0}{dz^2} + (1-Kz)\nabla^2\mathbf{u}_1 + KPrRe\frac{d\mathbf{u}_0}{dz}\left(\frac{\partial T_1}{\partial z} - \frac{\partial T_1}{\partial x}\right) - K\left(\frac{\partial \mathbf{u}_1}{\partial z} + \nabla w_1\right) + RaT_1\mathbf{k} \quad (9)$$

$$\nabla \cdot \mathbf{u} = 0 \quad (10)$$

$$\frac{\partial T_1}{\partial t} - w_1 + PrRe\,u_0(z)\frac{\partial T_1}{\partial x} = \nabla^2 T_1 \quad (11)$$

Table 1 Values of β_1, δ_1 and η_1 used in Eq. 8

Rigid - rigid		
Modified Couette flow		
$\beta_1 = 0$	$\delta_1 = 2$	$\eta_1 = -1$
Modified Poiseuille flow		
$\beta_1 = -12$	$\delta_1 = 12$	$\eta_1 = -2$
Modified returning flow		
$\beta_1 = -9$	$\delta_1 = 6$	$\eta_1 = 0$
Rigid-free		
Modified Couette flow		
$\beta_1 = 0$	$\delta_1 = 1$	$\eta_1 = -1/2$
Modified Poiseuille flow		
$\beta_1 = -3$	$\delta_1 = 6$	$\eta_1 = -2$
Modified returning flow		
$\beta_1 = -9$	$\delta_1 = 6$	$\eta_1 = 0$

At this point some differences between the governing Eqs. 10-11 and the Eqs. 4 presented by Cox (1997) can be noticed for the linear case. The system of Eqs. 10-11 show 5 modified terms which contribute importantly to the convective linear instability of the system. These terms and some others arising in the non-linear case are missing in the theory developed by Cox (1997). The mathematical operations were performed in the software MAPLE 16. Some calculations are not presented here because of the space but these can be obtained from the author upon request.

It is suitable to separate the pressure field from that of velocity so that $(\nabla\times)$ is operated twice on the Navier-Stokes Eq. 9. In the resulting equation the vertical component of the velocity is independent of the other two components. Next, the perturbed variables in the governing equations are expanded in normal modes as follows,

$$[w_1, T_1] = [W(z), \theta(z)]\exp[i(k_x x + k_y y) + \sigma t] \quad (12)$$

where $k = \sqrt{k_x^2 + k_y^2}$ is the wavenumber of the perturbation and σ is a complex parameter whose real part is the growth rate of the perturbations and its imaginary part is the frequency of oscillation. Thus, the governing Eqs. 10-11 become,

$$\left(D^2 - k^2\right)\left(D^2 - k^2 - \frac{\sigma}{Pr}\right)W = k^2 Ra\theta + \left[k^4 K - ik\cos(\gamma)Re\left(k^2 + D^2\right)u_0\right]W + k_x^2 KPrReD(\theta Du_0) + ik_x Reu_0 D^2 W + ik_x KPrRe\left(2D^2 u_0 D\theta + Du_0 D^2\theta\right) + K\left[2D\left(D^2 - k^2\right)W + zD^2\left(D^2 - 2k^2\right)W\right] \quad (13)$$

$$\left(D^2 - k^2 - \sigma - ik_x PrReu_0\right)\theta = -W \quad (14)$$

where $D = d/dz$. Notice that $k_x = k\cos(\gamma)$. The system of Eqs. 13-14 is subjected to thermal and mechanical boundary conditions. The thermal boundary conditions are those of poorly thermal conducting walls,

$$D\theta \pm B\theta = 0 \qquad at \qquad z = 0, 1 \quad (15)$$

where B is the Biot number. The boundary conditions for W in the case of both rigid walls are given in Eqs. 16 while for the case of free upper wall are given in Eq. 17,

$$W = DW = 0 \qquad at \qquad z = 0, 1 \quad (16)$$

$$W = D^2 W = 0 \qquad at \qquad z = 0, 1. \quad (17)$$

3. LINEAR STABILITY ANALYSIS

In this section the stability of the basic state to small perturbations is considered. Thus, the eigenvalue problem for Ra stated in Eqs. 13-14 subject to the boundary conditions Eqs. 15-17 shall be studied with the shallow layer theory (Cox 1997; Cox 1996; Dávalos-Orozco

and Manero 1986; Pismen 1986; Nayfeh 1981; Gertsberg and Sivashinsky 1981). As the bounding walls are poorly thermal conducting, the Biot number is taken $B = \varepsilon^2 \bar{B}$ with $\varepsilon << 1$. In this way, the following set of expansions is used for the variables and parameters appearing in Eqs. 13-14,

$$W = \varepsilon W_1 + \varepsilon^2 W_2 + \ldots \quad (18)$$

$$\theta = \theta_0 + \varepsilon\theta_1 + \varepsilon^2\theta_2 + \ldots \quad (19)$$

$$\sigma = \varepsilon^2\sigma_2 + \varepsilon^3\sigma_3 \ldots \quad (20)$$

$$Ra = Ra_0 + \varepsilon Ra_1 + \ldots \quad (21)$$

As mentioned above, in this problem only small temperature dependent viscosity effects are considered then $K = \varepsilon\bar{K}$. The two flow regimes corresponding to weak and strong shear are scaled in different ways each. In order to introduce the next scalings, similar arguments to those exposed by Cox (1997) are embraced. When the imposed shear flow is weak $Re = \sqrt{\varepsilon}R$ and $(k_x, k_y) = O(\sqrt{\varepsilon})$ are taken. This means that near the onset of convection for weak shear flows, stream-wise and cross-stream length scales are equal. Because the shear flow is weak, the system is allowed to provide the transition to the anisotropy in the length scales.

In the case of strong shear flow $Re = O(1)$, $k_x = O(\varepsilon)$ and $k_y = O(\sqrt{\varepsilon})$ are taken. When the shear flow is strong at the onset of convection the stream-wise spatial scale becomes greater than the cross-stream one. It should be remarked that the weak and strong nature of the flow is only assign to Re keeping $Pr = O(1)$ which differs from the analysis of Cox (1997). Besides, Pr and Re not always appear with equal powers in Eqs 13-14.

One important fact should be noted here. The Reynolds number Re was defined in terms of the maximum velocity U_{Max} of the fluid in the basic state and it is obvious the dependence of U_{Max} on K. As a consequence Re also depends on K. Fortunately, only small temperature dependent viscosity effects $K = O(\varepsilon)$ are considered in this investigation allowing and approximation of U_{Max}. For short, the influence of small K on Re is of $O(\varepsilon)$ making the assumptions of weak and strong shear flow valid.

The process of solution for this eigenvalue problem is now described. After substitution of the expansions Eqs. 18-21 and the proper scalings for weak or strong shear, systems of equations with their corresponding boundary conditions at different orders in ε are obtained. These systems of equations should be solved in a consecutive fashion.

3.1 Case of Weak Shear Flow. Rigid-rigid Boundaries

Firstly, the case of convection in the presence of weak shear flow in a fluid layer bounded by two rigid walls shall be considered. Thus, at $O(1)$ the following system of equations is obtained,

$$D^2\theta_0 = 0 \quad (22)$$

$$D^4 W_1 = Ra_0 \bar{k}^2 \theta_0 \quad (23)$$

subject to the following boundary conditions,

$$W_1 = DW_1 = 0 \quad at \quad z = 0, 1 \quad (24)$$

$$D\theta_0 = 0 \quad at \quad z = 0, 1 \quad (25)$$

At $O(\varepsilon)$ the problem is,

$$D^2\theta_1 - (\bar{k}^2 + iPrRu_0\bar{k}\cos(\gamma))\theta_0 = -W_1 \quad (26)$$

$$\begin{aligned} D^4 W_2 - 2\bar{k}^2 D^2 W_1 &+ i R\bar{k}\cos(\gamma)\left(W_1 D^2 u_0 \right. \\ \left. -u_0 D^2 W_1\right) = Ra_0\bar{k}^2\theta_1 &+ Ra_1\bar{k}^2\theta_0 \\ +\bar{K}\left(zD^4 - 2D^3\right)W_1 & \end{aligned} \quad (27)$$

subject to the following boundary conditions,

$$W_2 = DW_2 = 0 \quad at \quad z = 0, 1 \quad (28)$$

$$D\theta_1 = 0 \quad at \quad z = 0, 1 \quad (29)$$

At $O(\varepsilon^2)$ only the equation for θ_2 is necesary,

$$D^2\theta_2 - (\bar{k}^2 + iPrRu_0\bar{k}\cos(\gamma))\theta_1 + \sigma_2\theta_0 = -W_2 \quad (30)$$

subject to the following boundary conditions,

$$D\theta_2 \pm \bar{B}\theta_0 = 0 \quad at \quad z = 0, 1 \quad (31)$$

It should be remarked that at $O(\varepsilon^2)$ a solbavility condition must be satisfied in order to avoid a breakdown in the expansion (Nayfeh 1981). It has been considered that contributions at this order of approximation are enough for the linear stability analisys (Pismen 1986; Gertsberg

and Sivashinsky 1981). The solution to the systems of equations stated above can be easily obtained. Therefore, at $O(1)$,

$$\theta_0 = 1 \tag{32}$$

$$W_1 = \frac{Ra_0\bar{k}^2 z^2}{24}\left(z^2-2z+1\right) \tag{33}$$

where the θ_0 have been normalized. At $O(\varepsilon)$ θ_1 and W_2 can be calculated after substituion of θ_0 and W_1. Thus, for θ_1,

$$\theta_1 = -z^2(z-1)^2\left(z^2-z-\frac{1}{2}\right)\bar{k}^2 - z^2 i\bar{k}PrR\cos(\gamma)\left[\left(\beta+\frac{3}{2}\delta\right)\left(\frac{z^4}{3}-z^3\right)+\left(\frac{3}{4}\beta+\frac{5}{4}\delta\right)-\frac{\delta}{6}z-\frac{\eta}{2}\right] \tag{34}$$

Ra_0 was determined from the solvablity condition at $O(\varepsilon)$. In order to obtain solution Eq. 34 it was required that the integral, ranging from $z=0$ to $z=1$, of the inhomegeneus part vanished. Hence, $Ra_0 = 720$. The solution W_2 is not shown because it is a large expression but it can be obtain from the author upon request. Next, a second solvability condition must be satisfied at $O(\varepsilon^2)$. Integrating Eq. 30 across the fluid layer depth yields,

$$\sigma_2 = -2\bar{B}+\left(\frac{Ra_1}{720}+\frac{\bar{K}}{2}\right)\bar{k}^2-\frac{17}{462}\bar{k}^4 - \frac{29}{4620}i\bar{k}R\cos(\gamma)\left[\left(\left(\beta+\frac{60}{29}\delta\right)+\frac{275}{174}\beta+\frac{55}{29}\delta\right)\bar{k}^2-\frac{770}{29}Pr\bar{K}\left(\beta+\frac{3}{2}\delta\right)\right] - \frac{29}{2772}\bar{k}^2PrR^2\cos^2(\gamma)\left[\left(\beta^2+\frac{119}{58}\beta\delta+\frac{153}{145}\delta^2\right)Pr-\frac{155}{174}\left(\beta+\frac{6}{5}\delta\right)\left(\beta+\frac{3}{2}\delta\right)\right] \tag{35}$$

Since σ_2 is complex, the real part of Eq. 35 is the growth rate of the perturbation and the imaginary part corresponds to the frequency of oscillation. Reintroducing the unscaled parameters, the following expressions for the real and imaginary parts of σ_2 are obtained

$$\sigma_R = -2B+\left(\frac{Ra-720}{720}+\frac{K}{2}\right)k^2-\frac{17}{462}k^4 - \frac{29}{2772}PrRe^2k^2\cos^2(\gamma)\left[\left(\beta_1^2+\frac{153}{145}\delta_1^2+\frac{30}{29}\eta_1^2+\frac{119}{58}\beta_1\delta_1+\frac{133}{145}\beta_1\eta_1+\frac{30}{29}\eta_1\delta_1\right)Pr-\frac{11}{348}(5\beta_1+6\delta_1+12\eta_1)(2\beta_1+3\delta_1+6\eta_1)\right] \tag{36}$$

$$\omega = -\frac{2}{77}kRe\cos(\gamma)\left[\left(\left(\frac{29}{120}\beta_1+\frac{1}{2}\delta_1+\eta_1\right)Pr+\frac{55}{144}\beta_1+\frac{11}{24}\delta_1+\frac{11}{12}\eta_1\right)k^2-\frac{77}{4}PrK\left(\frac{1}{3}\beta_1+\frac{1}{2}\delta_1+\eta_1\right)\right] \tag{37}$$

where σ_R is the growth rate and ω is the frequency of oscillation. In Eqs. 36-37, the terms including K are modifications to the theory presented by Cox (1997) and these arise naturally when small changes of viscosity with temperature are taken into account. Ra is obtained from Eq. 36 by setting $\sigma_R = 0$,

$$Ra = 1440\frac{B}{k^2}+720-360K+\frac{2040}{77}k^2 - \frac{600}{77}PrRe^2\cos^2(\gamma)\left[\left(\frac{29}{30}\beta_1^2+\frac{51}{50}\delta_1^2+\eta_1^2+\frac{119}{60}\beta_1\delta_1+\delta_1\eta_1+\frac{133}{150}\beta_1\eta_1\right)Pr-\frac{11}{15}\left(\frac{5}{12}\beta_1+\frac{1}{2}\delta_1+\eta_1\right)\left(\frac{1}{3}\beta_1+\frac{1}{2}\delta_1+\eta_1\right)\right] \tag{38}$$

In this case $k_c = \sqrt[4]{924B/17}$ and Ra_c is obtained directly after substitution of k_c in Eq. 38. The critical frequency of oscillation ω_c is also calculated from substitution of k_c into Eq. 37. Ra_c and ω_c are not shown. It is noticeable that as the fluid viscosity changes with temperature the new contributions destabilize the system and this information is important in further non-linear analysis.

Figure 3 shows curves of criticality of the Rayleigh number Ra_c against Re. Embedded in Fig. 3. cells for convection in the absence of parallel shear flow and with Poiseuille shear flow are presented. These convective cells are presented to shown that the convection cells are neither broken nor larger since the shear flow does not affect the critical wavenumber. On the other hand, the magnitude of the critical Rayleigh number does change depending on the shear flow applied as shown by the curves of criticality.

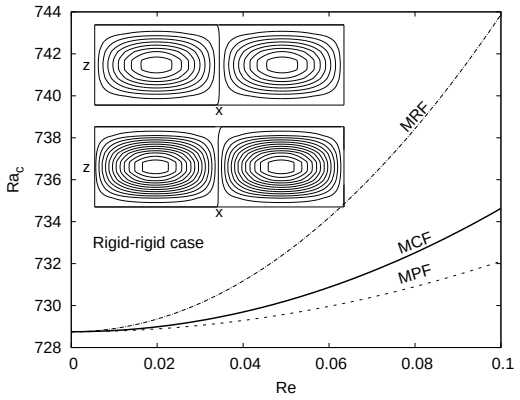

Fig. 3. Curves of criticality for case of weak shear. Dashed, solid and dot-dashed lines represent MPF, MCF and MRF, respectively. Convection cells at criticality are also shown from top to bottom for $Re = 0$ and MPF at $Re = 0.1$. In this case: $Pr = 7$, $B = 0.001$, $\gamma = 0$ and $K = 0.01$.

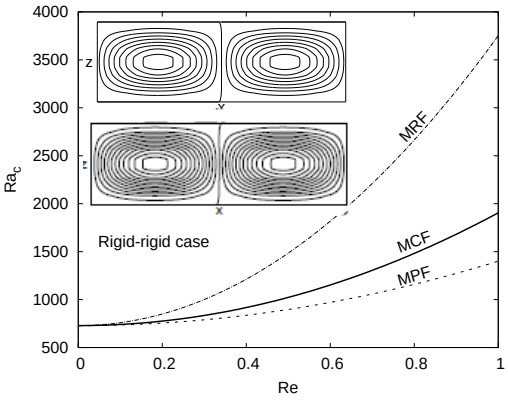

Fig. 4. Curves of criticality for case of strong shear. Dashed, solid and dot-dashed lines represent MPF, MCF and MRF, respectively. Convection cells at criticality are also shown from top to bottom for $Re = 0$ and MPF at $Re = 1$. In this case: $Pr = 7$, $B = 0.001$, $\gamma = 45$ and $K = 0.01$.

The applied process of calculation for this case can be easily followed to obtained σ_R and ω in the limit of strong shear flow. Besides, the case of rigid-free boundary conditions should also be made. Then, in order to save space only results are presented.

3.2 Case of strong shear flow. Rigid-rigid boundaries

In this case $Re = O(1)$, $k_x = O(\varepsilon)$ and $k_y = O(\sqrt{\varepsilon})$. Thus, the growth rate is given by,

$$\sigma_R = -2B + \left(\frac{Ra-720}{720} + \frac{K}{2}\right)k^2\sin^2(\gamma) - \frac{17}{462}k^4\sin^4(\gamma) - \frac{17}{1540}PrRe^2k^2\cos^2(\gamma)\left[\left(\frac{145}{153}\beta_1^2 + \delta_1^2 + \frac{50}{51}\eta_1^2 + \frac{35}{18}\beta_1\delta_1 + \frac{133}{153}\beta_1\eta_1 + \frac{50}{51}\eta_1\delta_1\right)Pr - \frac{55}{102}\left(\frac{2}{3}\beta_1 + \delta_1 + 2\eta_1\right)\left(\frac{5}{6}\beta_1 + \delta_1 + 2\eta_1\right)\right] \quad (39)$$

while the frequency of oscillation is,

$$\omega = -\frac{2}{77}kRe\cos(\gamma)\left[\left(\left(\frac{29}{120}\beta_1 + \frac{1}{2}\delta_1 + \eta_1\right)Pr + \frac{55}{144}\beta_1 + \frac{11}{24}\delta_1 + \frac{11}{12}\eta_1\right)k^2\sin^2(\gamma) - \frac{77}{4}PrK\left(\frac{1}{3}\beta_1 + \frac{1}{2}\delta_1 + \eta_1\right)\right] \quad (40)$$

In this case $k_c = (1/\sin(\gamma))\sqrt[4]{924B/17}$ and,

$$Ra_c = 720 - 360K + \frac{4080}{77}\sin^2(\gamma)k_c^2 - \frac{600}{77}PrRe^2\cos^2(\gamma)\left[\left(\frac{29}{30}\beta_1^2 + \frac{51}{50}\delta_1^2 + \eta_1^2 + \frac{119}{60}\beta_1\delta_1 + \delta_1\eta_1 + \frac{133}{150}\beta_1\eta_1\right)Pr - \frac{11}{15}\left(\frac{5}{12}\beta_1 + \frac{1}{2}\delta_1 + \eta_1\right)\left(\frac{1}{3}\beta_1 + \frac{1}{2}\delta_1 + \eta_1\right)\right] \quad (41)$$

The critical frequency of oscillation ω_c is not shown but can be calculated from substitution of k_c into Eq. 40. It can be easily seen that for $K = 0$ and $Re = 0$, the well known value 720 is recovered (Riahi 1985; Gertsberg and Sivashinsky 1981; Chapman and Proctor 1980a).

Figure 4 shows curves of critical Rayleigh numbers Ra_c against the Reynolds number Re for MPF, MCF and MRF. Besides, two embedded convection cells are also shown.

3.3 Case of weak shear flow. Rigid-free boundaries

In this case $Re = O(\sqrt{\varepsilon})$, $(k_x, k_y) = O(\sqrt{\varepsilon})$. Thus, the growth rate is given by,

$$\sigma_R = -2B + \left(\frac{Ra-320}{320} + \frac{5}{12}K\right)k^2 - \frac{58}{693}k^4 - \frac{8}{693}PrRe^2k^2\cos^2(\gamma)\left[\left(\frac{481}{864}\beta_1^2 + \frac{73}{160}\delta_1^2 + \eta_1^2 + \frac{577}{576}\beta_1\delta_1 - \frac{283}{1440}\beta_1\eta_1 - \frac{\eta_1\delta_1}{32}\right)Pr - \frac{33}{8}\left(\frac{125}{216}\beta_1 + \frac{5}{8}\delta_1 + \eta_1\right)\left(\frac{1}{3}\beta_1 + \frac{1}{2}\delta_1 + \eta_1\right)\right] \quad (42)$$

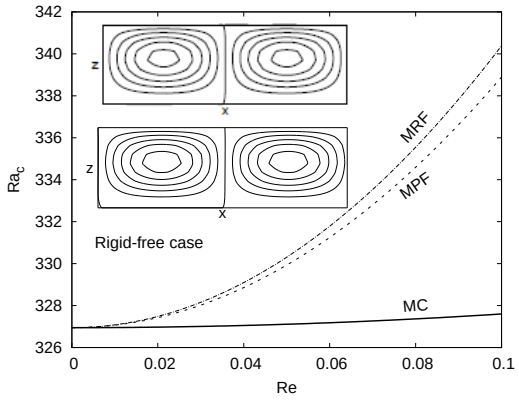

Fig. 5. Curves of criticality for the case of weak shear. Dashed, solid and dot-dashed lines represent MPF, MCF and MRF, respectively. Convection cells at criticality are from top to bottom for $Re = 0$ and MPF at $Re = 0.1$. In this case: $Pr = 7$, $B = 0.001$, $\gamma = 0$ and $K = 0.01$.

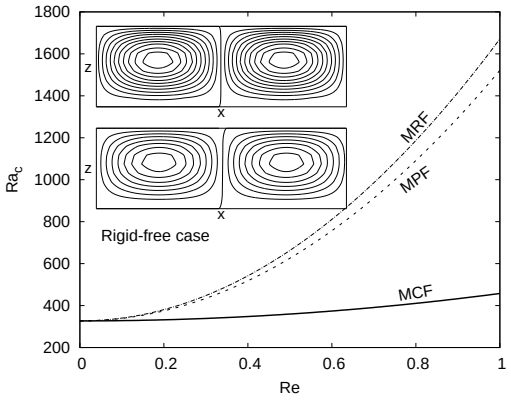

Fig. 6. Curves of criticality for the case of strong shear. Dashed, solid and dot-dashed lines represent MPF, MCF and MRF, respectively. Convection cells at criticality are also shown from top to bottom for $Re = 0$ and MPF at $Re = 1$. In this case: $Pr = 7$, $B = 0.001$, $\gamma = 45$ and $K = 0.01$.

while the frequency of oscillation is,

$$\omega = -\frac{50}{693}kRe\cos(\gamma)\left[\left(\left(\frac{4243}{9000}\beta_1+\frac{133}{200}\delta_1+\eta_1\right)Pr + \frac{55}{144}\beta_1+\frac{33}{80}\delta_1+\frac{33}{50}\eta_1\right)k^2 - \frac{237}{40}PrK\left(\frac{1}{3}\beta_1 + \frac{1}{2}\delta_1+\eta_1\right)\right] \tag{43}$$

In this case $k_c = \sqrt[4]{693B/29}$ and,

$$Ra_c = 320 - \frac{400}{3}K + \frac{37120}{693}k_c^2 - \frac{1168}{693}PrRe^2\cos^2(\gamma)\left[\left(\frac{2405}{1971}\beta_1^2+\delta_1^2+\frac{160}{73}\eta_1^2+\frac{2885}{1314}\beta_1\delta_1-\frac{5}{73}\delta_1\eta_1 - \frac{283}{657}\beta_1\eta_1\right)Pr - \frac{825}{292}\left(\frac{25}{27}\beta_1+\delta_1+\frac{8}{5}\eta_1\right)\left(\frac{2}{3}\beta_1+\delta_1+2\eta_1\right)\right] \tag{44}$$

The critical frequency of oscillation ω_c is not shown but can be calculated from substitution of k_c into Eq. 43. Curves of criticality for the different parallel flows in the weak shear approximation are presented in Fig. 5. Notice that the two embedded convective cells, $Re = 0$ and $Re = 0.1$, are very similar since the shear flow is weak.

3.4 Case of Strong Shear Flow. Rigid-free Boundaries

In this case $Re = O(1)$, $k_x = O(\varepsilon)$ and $k_y = O(\sqrt{\varepsilon})$. Thus, the growth rate is given by,

$$\sigma_R = -2B + \left(\frac{Ra-320}{320}+\frac{5}{12}K\right)k^2\sin^2(\gamma) - \frac{58}{693}k^4\sin^4(\gamma) - \frac{8}{693}PrRe^2k^2\cos^2(\gamma)\left[\left(\frac{481}{694}\beta_1^2 + \frac{73}{160}\delta_1^2+\eta_1^2+\frac{577}{576}\beta_1\delta_1-\frac{283}{1440}\beta_1\eta_1-\frac{\eta_1\delta_1}{32}\right)Pr - \frac{33}{8}\left(\frac{125}{216}\beta_1+\frac{5}{8}\delta_1+\eta_1\right)\left(\frac{1}{3}\beta_1+\frac{1}{2}\delta_1+\eta_1\right)\right] \tag{45}$$

while the frequency of oscillation is,

$$\omega = -\frac{50}{693}kRe\cos(\gamma)\left[\left(\left(\frac{4243}{9000}\beta_1+\frac{133}{200}\delta_1+\eta_1\right)Pr + \frac{55}{144}\beta_1+\frac{33}{80}\delta_1+\frac{33}{50}\eta_1\right)k^2\sin^2(\gamma) - \frac{237}{40}PrK\left(\frac{1}{3}\beta_1+\frac{1}{2}\delta_1+\eta_1\right)\right] \tag{46}$$

In this case $k_c = (1/\sin(\gamma))\sqrt[4]{693B/29}$ and,

$$Ra_c = 320 - \frac{400}{3}K + \frac{37120}{693}k_c^2\sin^2(\gamma) - \frac{1168}{693}PrRe^2\cos^2(\gamma)\left[\left(\frac{2405}{1971}\beta_1^2+\delta_1^2+\frac{160}{73}\eta_1^2 + \frac{2885}{1314}\beta_1\delta_1-\frac{5}{73}\delta_1\eta_1-\frac{283}{657}\beta_1\eta_1\right)Pr - \frac{825}{292}\left(\frac{25}{27}\beta_1+\delta_1+\frac{8}{5}\eta_1\right)\left(\frac{2}{3}\beta_1+\delta_1+2\eta_1\right)\right] \tag{47}$$

The critical frequency of oscillation ω_c is not shown but can be calculated from substitution

of k_c into Eq. 46. Curves of criticality for the different parallel flows in the strong shear approximation are presented in Fig. 6.

4. RESULTS

In the previous section analytical expressions describing the linear stability of the system were shown for a number of cases. Among all the results, the terms accounting for temperature dependent viscosity contributions are of interest because these ones facilitate the destabilization of the fluid layer. Although more contributions due to the temperature dependence of viscosity, through the basic state u_0, are possible these would be small according to the approximation $K = O(\varepsilon)$. All mathematical expressions for Ra_c show similar quadratic dependence on Re and for all cases the critical Rayleigh number Ra_c increases with the shear flow, Re. Other findings on the velocity profiles deserve to be mentioned as contribution to the theory of Cox (1997) since u_0 is changed with K contributions. Found results were compared with others reported in the literature. For example, for $B = 0$ and $Re = 0$, Ra_c reduces to well known value 720 for the case of rigid-rigid boundaries (Riahi 1985; Gertsberg and Sivashinsky 1981; Chapman and Proctor 1980a) and to 320 for the case of rigid-free-boundaries (Chapman and Proctor 1980a; Sparrow et al. 1964). Another important fact is that shear flows and temperature dependent viscosity effects have opposite impact in the stability of the system.

4.1 Consequences in the non-Linear Stability

In this section attention is paid to non-linear terms arising in the governing equations of this problem. These non-linear terms appear naturally when considering the temperature dependence of viscosity from the beginning in the constitutive equation as made by Wall and Wilson (1996) and Chung and Wulandana (2006). These contributed terms were omitted in the theory developed by Cox (1997) and could be of paramount importance in the pattern selection problem. These mathematical expressions are not shown here for being out of the scope of this paper. However, from the present analysis it can be said that the quadratic terms along with the modified parallel shear flow profiles are an improvement.

5. CONCLUSIONS

The problem of forced convection in a infinite horizontal Newtonian fluid layer bounded by two poorly conducting walls was studied here. Also, small variations of viscosity with temperature were taken into account. Main results of this work point to updating and extending previous studies reported in the literature.

First, the inclusion of temperature dependence of viscosity in the fluid constitutive equation gave rise to new terms which are important in the linear stability analysis. The effect of the parameter K, accounting for slight temperature dependence of the viscosity, was destabilizing in all cases presented here. For the case of rigid-rigid boundaries changes in the viscosity decrease the stability parameter Ra_c through the term $-360K$ and through $-400K/3$ for case of rigid-free boundary conditions, respectively. The destabilizing effect becomes more important when both walls are solid that when the upper boundary is open to the ambient. This may occur due to the asymmetry in the boundary conditions which physically implies less friction in the case of upper boundary open to the ambient. These destabilizing terms coming from the viscous term in the Navier-Stokes equations are contributed by the perturbed fluid velocity which is smaller when the upper surface is free.

Second, the imposed shear flows stabilize the system. In other words, for fixed K the smallest Ra_c is achieved when $Re = 0$. On the other hand, forced convection sets in always as oscillatory motions in all considered cases and stationary convection may appear when $Re = 0$. A possible mechanism through which the shear flow may stabilize oscillatory motions is by dragging the uprising heated fluid in the horizontal direction. Thus, the portion of fluid may experience heat loss before achieving the top surface. Summarizing, the imposed shear flows and temperature dependence of viscosity have opposite effects on the thermoconvective stability of the fluid layer, since the first ones are stabilizers and the second one are destabilizers.

Another important result is that the fluid layer may be stabilized by making the angle orientation $\gamma = 90$. This is equivalent to set $Re = 0$ since when $\gamma = 90$ the frequency of oscillation vanishes too. From all imposed shear flows the most unstable was that of MPF, then that of MCF and finally that of MRF for rigid-rigid boundaries. For rigid-free boundaries, from all imposed shear flows the most unstable was that of MCF, then that of MPF and finally that of MRF. The previous Couette and Poiseuille flow, considered by (Cox 1997), were no longer possible since the temperature dependent viscosity modifies the velocity profiles. The linear

theory of this problem was also complemented with a third imposed shear flow characterized by its returning feature. Also, with the help of a short computation including the non-linear terms of this problem it have been foreseen that some non-linear contributions including K may become important to the understanding of this problem.

The present paper introduced some improvements to the theory of linear stability of convection forced convection. In the light of these results a more broad non-linear stability analysis shall be carried out in a future work. Also, the problem with perfect heat conducting walls deserves attention.

ACKNOWLEDGEMENTS

The author thanks to the Programa de Mejoramiento del Profesorado (PROMEP) for founding support.

A BASIC STATE VELOCITY PROFILES

In this appendix, analytical expressions for the basic state velocity profiles are given. Notice that these expressions are not approximated and non-dimensionalized.

A1 MPF with rigid-rigid boundary conditions

$$u_0 = \frac{\left(2z+1-2K^{-1}\right)\ln\left(1-K\right)-2\left(1+\ln\left(1-Kz\right)\right)}{2\ln\left(-K^{-1}\ln\left(1-K\right)\right)+\ln\left(1-K\right)} \tag{48}$$

A2 MPF with rigid-free boundary conditions

$$u_0 = \frac{A_1+2K(K-1)\ln(1-Kz)+K^2(3K-2z)}{2(K-1)\ln(1-K)+K(K-2)} \tag{49}$$

with

$$A_1 = -2(K-1)^2\ln(1-K)-2K \tag{50}$$

A3 MCF with rigid-rigid boundary conditions

$$u_0 = \frac{-K\ln\left(1-Kz\right)+\left(K-1\right)\ln\left(1-K\right)}{K+\left(1-K\right)\ln\left(1-K\right)} \tag{51}$$

A4 MCF with rigid-free boundary conditions

$$u_0 = \frac{1}{K^2}\left(K(K-1)\left[1+\ln(1-Kz)\right] -(K-1)^2\ln(1-K)\right) \tag{52}$$

A5 MRF with rigid-rigid boundary conditions

$$u_0 = \frac{K\left[2z(K-1)\ln(1-K)-2zK-K\ln(1-Kz)\right]}{2(K-1)\ln(1-K)-2K-A_2} \tag{53}$$

with

$$A_2 = K^2\left[\ln\left(\frac{K^2}{K+(1-K)\ln(1-K)}\right)-\ln(2)-1\right] \tag{54}$$

A6 MRF with rigid-free boundary conditions

$$u_0 = \frac{K\left[2z(K-1)\ln(1-K)-2zK-K\ln(1-Kz)\right]}{2(K-1)\ln(1-K)-2K-A_3} \tag{55}$$

with

$$A_3 = K^2\left[\ln\left(\frac{K^2}{K+(1-K)\ln(1-K)}\right)-\ln(2)-1\right] \tag{56}$$

In all velocity profiles shown in this appendix the small parameter ε has been erased and K is used instead of $\bar{K}$. Finally, Table 2 shows data to complement those presented in Table 1 These parameter values are important to generate the velocity profiles shown in Fig. 2. Eqs. 48, 51 and 53 are plotted and presented earlier in the section 2 as Figs. 2a-2c.

Table 2 Values of β_2, δ_2, η_2 and ϕ_0 used in Eq. 8

Rigid - rigid			
Modified Couette flow			
$\beta_2=0$	$\delta_2=1$	$\eta_2=-2/3$	$\phi_2=0$
Modified Poiseuille flow			
$\beta_2=-8$	$\delta_2=12$	$\eta_2=-4$	$\phi_2=0$
Modified returning flow			
$\beta_2=-6$	$\delta_2=7$	$\eta_2=-5/3$	$\phi_2=0$
Rigid-free			
Modified Couette flow			
$\beta_2=0$	$\delta_2=1/2$	$\eta_2=-1$	$\phi_2=1/3$
Modified Poiseuille flow			
$\beta_2=-2$	$\delta_2=-9/2$	$\eta_2=-3$	$\phi_2=1/2$
Modified returning flow			
$\beta_2=-6$	$\delta_2=7$	$\eta_2=-5/3$	$\phi_2=0$

REFERENCES

Alikina, O. N. and E. L. Tarunin (2001). Subcritical motions of a fluid with temperature-dependent viscosity. *Fluid Dyn. 36*(4), 574–580.

Alloui, Z., N. B. Khelifa, H. Beji, P. Vasseur, and A. Guizani (2013). The onset of convection of power-law fluids in a shallow cavity heated from below by a constant heat flux. *J. Non-Newtonian Fluid Mech. 196*, 70–82.

Bassou, N. Rharbi, Y. (2009). Role of Bénard–Marangoni instabilities during solvent evaporation in polymer surface corrugations. *Langmuir 25*, 624–632.

Bessonov, O. A., V. A. Brailovskaya and B. Roux (1998). Numerical modeling of three-dimensional shear flow in a cavity with moving lids. *Fluid Dyn. 33*(3), 331–337.

Busse, F. H. and N. Riahi (1980). Nonlinear convection in a layer with nearly insulating boundaries. *J. Fluid Mech. 96*(02), 243–256.

Chapman, C. J. and M. R. E. Proctor (1980a). Nonlinear Rayleigh–Bénard convection between poorly conducting boundaries. *J. Fluid Mech. 101*(4), 759–782.

Chapman, C. J. Childress, S. and M. R. E. Proctor (1980b). Long wavelength thermal convection between non-conducting boundaries. *Earth Plane. Sci. Let. 51*(2), 362–369.

Chung, B. J. Vaidya, A. and R. Wulandana (2006). Stability of steady flow in a channel with linear temperature dependent viscosity. *Int. J. Appl. Math and Mech. 2*, 24–33.

Cox, S. M. (1996). The onset of thermal convection between poorly conducting horizontal boundaries in the presence of a shear flow. *SIAM J. Appl. Math. 56*(5), 1317–1328.

Cox, S. M. (1997). Long-wavelength thermal convection in a weak shear flow. *IMA J. Appl. Math. 58*, 159–184.

Dávalos-Orozco, L. A. and O. Manero (1986). Thermoconvective instability of a second-order fluid. *J. Phys. Soc. Jpn. 55*(2), 442–445.

Gertsberg, V. L. and G. I. Sivashinsky (1981, October). Large cells in nonlinear Rayleigh–Bénard convection. *Prog. Theor. Phys. 66*(4), 1219–1229.

Ghosh, S. K., G. C. Shit, and J. C. Misra (2014). Heat transfer in hydromagnetic fluid flow: study of temperature dependence of fluid viscosity. *J. Applied Fluid Mech. 7*(4), 633–640.

Höink, T. and A. Lenardic (2010). Long wavelength convection, Poiseuille–Couette flow in the low-viscosity asthenosphere and the strength of plate margins. *Geophys. J. Int. 180*, 23–33.

Howle, L. E. (1997a). Active control of Rayleigh–Bénard convection. *Phys. Fluid 9*(7), 1861–1863.

Howle, L. E. (1997b). Control of Rayleigh–Bénard convection in a smaal aspect ratio container. *Int. J. Heat Mass Transfer 40*(4), 817–822.

Howle, L. E. (2000). The effect of boundary properties on controlled Rayleigh–Bénard convection. *J. Fluid Mech. 411*, 39–58.

Kameyama, M., H. Ichikawa, and A. Miyauchi (2013). A linear stability analysis on the onset of thermal convection of a fluid with strongly temperature-dependent viscosity in a spherical shell. *Theor. Comp. Fluid Dyn. 27*, 21–40.

Khalid, I. K., N. F. M. Mokhar, and N. M. Arifin (2013). Rayleigh-Benard convection in micropolar fluid with feedback control effect. *World App. Sci. J. 21*, 112–118.

Landuyt, W. and G. Ierley (2012). Linear stability analysis of the onset of sublithospheric convection. *Geophys. J. Int. 189*, 19–28.

Lappa, M. (2010). *Thermal Convection: Patterns, Evolution and Stability* (First ed.). Cambridge, USA: John Wiley and Sons.

Li, M. L., S. XU, and E. Kumacheva (2000). Convection in polymeric fluids subjected to vertical temperature gradients. *Macromolec. 33*, 4972–4978.

Li, M. L., S. Xu, and E. Kumacheva (2000). Convection patterns trapped in the solid state by UV–induced polymerization. *Langmuir 16*, 7275–7278.

Molla, M. M., S. C. Saha, and M. A. Hossain (2012). The effect of temperature dependent viscosity in MHD natural convectionn from an isothermal sphere. *J. Applied Fluid Mech. 5*(2), 25–31.

Nayfeh, A. H. (1981). *Introduction to Perturbation Techniques*. New York, USA: John Wiley and Sons, Inc.

Nicolas, X. (2002). Bibliographical review on the Poiseuille-Rayleigh-Bénard flows: the mixed convection flows in horizontal rectangular ducts heated from below. *Int. J. Thermal Sci. 41*, 961–1016.

Nie, Z. Kumacheva, E. (2008). Patterning surfaces with functional polymers. *Nat. 7*, 277–290.

Nikitin, S. A., D. S. Pavlovskii, and V. I. Polezhaev (1996). Stability and spatial structure of convection in an elongated horizontal layer with lateral heating. *Fluid Dyn. 31*(4), 503–510.

Ortiz–Pérez, A. S. and L. A. Dávalos–Orozco (2011). Convection in a horizontal fluid layer under an inclined temperature gradient. *Phys. Fluids 23*, 084107.

Ortiz–Pérez, A. S. and L. A. Dávalos–Orozco (2014). Convection in a horizontal fluid layer under an inclined temperature gradient for prandtl numbers $pr > 1$. *I. J. Heat Mass Transfer 68*, 444–455.

Palm, E., T. Ellingsen, and B. Gjevik (1967). On the occurrence of cellular motion in Bénard convection. *J. Fluid Mech. 30*, 651–661.

Pismen, L. M. (1986). Inertial effects in long-scale thermal convection. *Phys. Lett. A 116*(5), 241–244.

Riahi, N. (1985). Nonlinear thermal convection with finite conducting boundaries. *J. Fluid Mech. 152*, 113–123.

Sakurai, S., C. Furukawa, A. Okutsu, A. Miyoshi, and S. Nomura (2002). Control of mesh pattern of surface corrugation via rate of solvent evaporation in solution casting of polymer film in the presence of convection. *Polymer 43*, 3359–3364.

Sassos, A. and A. Pantokratoras (2011). Convection in the Rayleigh-Bénard flow with all fluid properties variable. *J. Thermal Sci. 20*(20), 454–459.

Schwartz, L. W., R. V. Roy, R. R. Eley, and S. Petrash (2001). Dewetting patterns in a drying liquid film. *J. Colloid Interface Sci. 234*, 363–374.

Sparrow, E. M., R. J. Goldstein, and V. K. Jonsson (1964). Thermal instability in a horizontal fluid layer: effect of boundary conditions and non-linear temperature profile. *J. Fluid Mech. 18*, 513–528.

Tang, J. and H. H. Bau (1993). Stabiization of the non-motion state in Rayleigh–Bénard convection through the use of feedback control. *Phys. Rev. Lett. 70*(12), 1795–1798.

Tang, J. and H. H. Bau (1994). Stabiization of the non-motion state in the Rayleigh–Bénard problem. *Proc. R. Soc. Lond. A 447*, 587–607.

Tang, J. and H. H. Bau (1998). Experiments on the stabiization of the non-motion state of a fluid layer heated from below and cooled from above. *J. Fluid Mech. 363*, 153–171.

Uguz, K. E. and R. Narayanan (2012). Instability in evaporative binary mixtures. II. the effect of Rayleigh convection. *Phys. Fluids 24*, 094102.

Wall, D. P. and M. Nagata (2000). Nonlinear equilibrium solutions for the channel flow of fluid with temperature-dependent viscosity. *J. Fluid Mech. 406*, 1–26.

Wall, D. P. and S. K. Wilson (1996). The linear stability of channel flow of fluid with temperature-dependent viscosity. *J. Fluid Mech. 323*, 107–132.

Weber, J. E. (1973). On thermal convection between non-uniformly heated planes. *Int. J. Heat Mass Transfer 16*(5), 961–970.

Xu, S. Kumacheva, E. (2002). Ordered morphologies in polymeric films produced by replication of convection patterns. *J. Am. Chem. Soc. 124*(7), 1142–1143.